

A RIEMANNIAN MODEL OF REGIONAL DEGENERATION OF THE HIPPOCAMPUS IN ALZHEIMER'S DISEASE

Xiuwen Liu¹, Yonggang Shi², Ying Wang¹, Paul M. Thompson², Washington Mio³

¹Department of Computer Science, Florida State University, Tallahassee, FL 32306

²Laboratory of NeuroImaging, UCLA School of Medicine, Los Angeles, CA 90095

³Department of Mathematics, Florida State University, Tallahassee, FL 32306

ABSTRACT

We develop a Riemannian model of shape of solids in 3D space to map and compare localized hippocampal atrophy in normal aging, conversion to Alzheimer's disease (AD), and progression of the disorder over a 1-year period. The study is based on magnetic resonance scans of 428 subjects acquired 12 months apart by the Alzheimer's Disease Neuroimaging Initiative. Shape geodesics are used to model the spatiotemporal evolution of the anatomy of the hippocampus of each subject and to uncover regional differences in shape that are characteristic of the three dynamical processes. We identify regions where changes in shape due to neurodegeneration in conversion to AD differs significantly from normal aging suggesting potential morphological markers of incipient AD.

Index Terms— Shape space, Alzheimer's disease, hippocampus, ADNI.

1. INTRODUCTION

Alzheimer's disease (AD) is a progressive disorder that currently afflicts millions of elderly individuals worldwide, with symptoms that evolve from an initial mild memory loss to a decline in all cognitive functions. As the hippocampus (HC) is one of the first parts of the brain to degenerate in AD, many brain imaging studies have focused on quantifying global and regional hippocampal volume loss and analyzing correlations with other measures of cognitive impairment; cf. [1, 2, 3] and references therein. Although global hippocampal volume loss in AD is well documented (cf. [3]), it is important to map the local atrophic patterns and model the dynamics of neurodegeneration in order to uncover morphological signatures that are specific to AD and can help in the early detection of the disorder, as well as to differentiate AD from other types of dementia.

In this paper, we develop a Riemannian model of spatiotemporal evolution of hippocampal shape over a 1-year time in normal aging, conversion to AD, and progression

of the disease with the goal of finding morphological characteristics that can help to track the disease with imaging methods. This study is based on longitudinal data collected by the Alzheimer's Disease Neuroimaging Initiative (ADNI) [4] and uses the shape of the full volume of the hippocampus extracted from magnetic resonance (MR) scans of 428 subjects acquired at two points in time, twelve months apart (see Table 1). In large scale studies such as the ADNI, the acquisition of multiple scans of all subjects over one year to accurately model the time evolution is not feasible, so the problems of interpolating a sparse set of observations and quantifying shape differences in a principled manner are of primary importance.

The shape model of spherical surfaces in 3D space of [5] could be used for the analysis of the contour surfaces of the hippocampus. A study along these lines was carried out in [6] with a different model of shape of surfaces. However, the study of the full hippocampal volume can potentially reveal shape features that are more sensitive to the structural differences in normal and AD brains, as well as more specific to AD. Thus, we propose a new model that extends that of [5] to shape of solids in 3D space and apply it to the study of the entire volume of the hippocampus. We use this Riemannian model to construct statistical maps of regional hippocampal atrophy in subjects with mild cognitive impairment (MCI), AD subjects, and healthy normal (NL) age-matched controls. Although MCI does not always evolve to AD, it is regarded as a transitional stage since, as a group, MCI subjects exhibit a 5-fold increased risk of conversion. Following a common practice, we first fix the hippocampus of a normal control as a reference and register the contour surfaces of the HC of all subjects with it using the techniques of [7]. We then use a thin-plate-spline interpolant [8] to extend the registration of the contour surfaces to the entire hippocampal volumes. Next, we use a subset of 50 normal controls to construct a hippocampal atlas as the mean shape of this subgroup. By construction, the HC of all subjects are already registered with the atlas, which is now used as the reference anatomy. We use the voxels of the atlas to obtain a (regular) cubical mesh representing its shape and transfer this mesh structure to

This research was supported in part by NSF grant DMS-0713012 and NIH Roadmap for Medical Research grant U54 RR021813.

# of Subjects	Baseline	Follow-up	Group Label	Index Range	Index Set
134	NL	NL	1	1–134	Λ_1
169	MCI	MCI	2	135–303	Λ_2
42	MCI	AD	3	304–345	Λ_3
83	AD	AD	4	346–428	Λ_4

Table 1. Breakdown of ADNI subjects included in this study according to diagnoses at baseline and follow-up scans. The total number of subjects is $N = 428$.

all other shapes via the volume registration. Hence, all shapes have a common underlying (abstract) mesh structure K inherited from the atlas. For each subject, we interpolate the meshes M_b and M_f extracted from the baseline and the 12-month follow-up scans, respectively, using volumetric shape geodesics.

We are interested in quantifying the dynamical behavior of the hippocampal volumes, particularly, the regional morphological changes over the 1-year period. The geodesic distance between the baseline and follow-up shapes gives a preliminary quantifier. However, this is a global measurement of shape change and does not reveal particular regions of interest. To achieve this, the key observation is that the square of the geodesic distance between two shapes has a natural interpretation as the (minimal) energy needed to morph a shape into another and this energy is an integration of local contributions. As such, the model provides a richer profile of local energies that we refer to as the *energy profile function* (EPF) associated with the geodesic. The quantification and comparison of group differences will be based on a statistical analysis of these EPFs. As all shapes are already registered with the atlas, we can pull back the EPF of each subject to the atlas, which gives a common domain for the comparison of different individuals and groups. We carry out a voxel-by-voxel analysis of the energy profile functions to identify the regions where shape changes in normal aging over a 1-year period differs significantly from those observed in the MCI-MCI, MCI-AD and AD-AD groups.

The paper is organized as follows. The geodesic model of shape used to estimate and quantify shape evolution is discussed in Section 2. Energy profile functions are introduced in Section 3 as a localization tool to quantify regional morphological changes. Section 4 presents a comparison of normal aging with the 1-year dynamics of MCI-MCI, MCI-AD and AD-AD, including statistical maps of group differences.

2. SHAPE OF SOLIDS IN 3D SPACE

Motivated by the shape data that we propose to analyze, we fix a reference cubical complex K and consider parametric shapes $\alpha: K \rightarrow \mathbb{R}^3$, where \mathbb{R}^3 denotes 3-dimensional Euclidean space. As we are interested in the hippocampus,

we assume that the topology underlying K is that of a solid bounded by a spherical surface. We also assume that α is an affine map on each cube of the complex K . Our Riemannian model uses a shape representation derived from the discrete exterior derivative of α . A representation based on the derivative is appealing because it is more sensitive to local non-linear deformations of shape such as regional shrinkage due to tissue loss. The usual derivative measures infinitesimal variations of a mapping, so the natural discrete analogue is the variation of α as we traverse an edge. Thus, the exterior derivative $d\alpha$ is defined on the oriented edges of K . Fix an arbitrary orientation for each edge of K and let $E = \{e_1, \dots, e_m\}$ be the resulting oriented edge set. If we denote the initial and terminal vertices of e_i by e_i^- and e_i^+ , respectively, then

$$d\alpha(e_i) = \alpha(e_i^+) - \alpha(e_i^-). \quad (1)$$

It suffices to consider a fixed orientation for each edge because reversal of orientation simply changes the sign of $d\alpha(e_i)$. Using a log-polar representation, we express the modular and directional components of $d\alpha(e_i)$ as

$$r_i = \log \|d\alpha(e_i)\| \quad \text{and} \quad v_i = d\alpha(e_i) / \|d\alpha(e_i)\|, \quad (2)$$

so that $d\alpha(e_i) = e^{r_i} v_i$. If we write $v_i^T = [v_{i1} \ v_{i2} \ v_{i3}]$, where T denotes transposition, the shape α is represented by the pair (r, v) with

$$r = \begin{bmatrix} r_1 \\ \vdots \\ r_m \end{bmatrix} \quad \text{and} \quad v = \begin{bmatrix} v_{11} & v_{12} & v_{13} \\ \vdots & \vdots & \vdots \\ v_{m1} & v_{m2} & v_{m3} \end{bmatrix}. \quad (3)$$

Not every pair (r, v) represents a discrete derivative, so we discuss the constraints they should satisfy. For each oriented cycle C in K , let n_i be the net number of times that the oriented edge e_i is traversed by C , where a negative sign indicates reversal of orientation. Then, pairs (r, v) that represent shapes are exactly those for which $\sum_{i=1}^m n_i e^{r_i} v_i = 0$. Intuitively, this simply means that (r, v) represents the derivative of some α if and only if its integral vanish along any cycle. Because of the simple topological type of K , one can show that it suffices to check these vanishing conditions along the

cycles of length 4 arising as the boundaries of the oriented faces of the cubes of K . Even among those, there is a high amount of redundancy. To obtain a minimal set of essential 4-cycles, we proceed as follows. Orient each face arbitrarily and denote them f_1, \dots, f_k . Form the $m \times k$ (boundary) matrix B , whose (i, j) -entry is ± 1 if the edge e_i is on the boundary of f_j , with the sign determined by the orientation. The entry is set to 0, otherwise. The pivot columns of B give a minimal set of independent 4-cycles. More precisely, if the j th column of B is a pivot column, we select the oriented 4-cycle representing the boundary of f_j .

We develop a shape model that is sensitive to scale because, among other things, we are interested in relative size changes associated with neurodegeneration. The fundamental ingredient of a Riemannian model is the quantification of the energy cost of an infinitesimal deformation (h, w) of a pair (r, v) because globalization of this measure of energy expenditure can be done via integration. In the model we propose, this energy cost is given by

$$\|(h, w)\|_{(r, v)}^2 = \sum_{i=1}^m h_i^2 e^{r_i} + \sum_{i=1}^m \|w_i\|^2 e^{r_i}. \quad (4)$$

Note that (4) is the sum of Euclidean contributions of individual edges weighted by their lengths e^{r_i} . Let the pairs (r, v) and (r^*, v^*) represent parametric shapes α and α^* , respectively. Given a path $\gamma(t) = (r(t), v(t))$, $0 \leq t \leq 1$, connecting (r, v) to (r^*, v^*) , the energy of the path is defined as

$$E(\gamma) = \int_0^1 \|(\partial_t r(t), \partial_t v(t))\|_{\gamma(t)}^2 dt. \quad (5)$$

Paths of minimal energy correspond to minimal length geodesics. We use constrained energy minimization to construct geodesics and calculate geodesic distances. We denote the distance $\delta((r, v), (r^*, v^*))$. Integrating each $(r(t), v(t))$ to a parametric mesh $\alpha_t: K \rightarrow \mathbb{R}^3$, one obtains a 1-parameter family of meshes representing the geodesic from (r, v) to (r^*, v^*) . As the integral is only defined up to an additive constant, we center each α_t to standardize the choice.

Since the (r, v) -representation of a shape is invariant under translations, to make the model invariant to general rigid transformations, it remains to account for the effect of orthogonal mappings. If s and s^* are the shapes represented by (r, v) and (r^*, v^*) , the (parametric) shape distance is defined as

$$\begin{aligned} d(s, s^*) &= \min_{U, V \in O(3)} \delta((r, vV^T), (r^*, v^*U^T)) \\ &= \min_{U \in O(3)} \delta((r, v), (r^*, v^*U^T)), \end{aligned} \quad (6)$$

where $O(3)$ is the group of 3×3 orthogonal matrices. Clearly, rigid transformations only affect the directional component of (r, v) , as indicated in (6). The second equality in (6) follows from the fact that orthogonal transformations preserve shape distance.

3. ENERGY PROFILE FUNCTIONS

A (parametric) geodesic $\gamma(t) = (r(t), v(t))$, $0 \leq t \leq 1$, is traversed with constant speed ω , where ω is the length of γ . Thus, the energy of γ is

$$E(\gamma) = \int_0^1 \|\partial_t \gamma(t)\|_{\gamma(t)}^2 dt = \omega^2. \quad (7)$$

On the other hand, we may write the energy as

$$E(\gamma) = \sum_{i=1}^m \int_0^1 \left(|\partial_t r_i(t)|^2 e^{r_i(t)} + \|\partial_t v_i(t)\|^2 e^{r_i(t)} \right) dt, \quad (8)$$

which expresses $E(\gamma)$ as a sum of the contributions of the individual edges. Thus, the *energy profile function* (EPF) defined as

$$\psi(e_i) = \int_0^1 \left(|\partial_t r_i(t)|^2 e^{r_i(t)} + \|\partial_t v_i(t)\|^2 e^{r_i(t)} \right) dt \quad (9)$$

quantifies the contribution of each edge to the total geodesic deformation energy. Although geodesic distance is a global quantifier of shape difference, the EPF provides a means to measure local shape differences and identify the regions where shape similarity and divergence are most pronounced. One may modify ψ to a function defined on the vertex set by letting the value on a vertex be the average value of ψ on the edges incident with that vertex. This is the variant we adopt.

4. COMPARISON WITH NORMAL AGING

In this section, we carry out a statistical comparison of the energy profile functions for the normal controls and the subjects in the MCI-MCI, MCI-AD and AD-AD groups. For each voxel x of the atlas, let $\psi_\ell(x)$ represents the value of the EPF of the geodesic that interpolates the baseline and follow-up observations for subject ℓ . Here, we use the fact that all shapes are registered with the atlas. For each x , we compare the distribution of the value of the EPFs at x in the normal aging group with the corresponding distributions for the MCI-MCI, MCI-AD, and AD-AD groups. In other words, we compare the distribution of $\{\psi_\ell(x), \ell \in \Lambda_1\}$ with the distributions of $\{\psi_\ell(x), \ell \in \Lambda_i\}$, $2 \leq i \leq 4$. (The index sets Λ_i are explained in Table 1.) Since one of the main objectives is to characterize the regions where shape changes over one year in these groups differ significantly from normal aging, we use a directional permutation t -test to compare NL-NL with each of the other groups. The percentage of voxels on the left hippocampus where the p -value is ≤ 0.05 for the MCI-MCI, MCI-AD, and AD-AD groups are 1.6%, 0.1% and 23.5%, respectively. For the right hippocampus, 6.2%, 1.7% and 7.7%. To visualize the regions of significance, we sectioned the volumetric atlases along 3 planes. Figure 1 shows the maps of p -values along these sections.

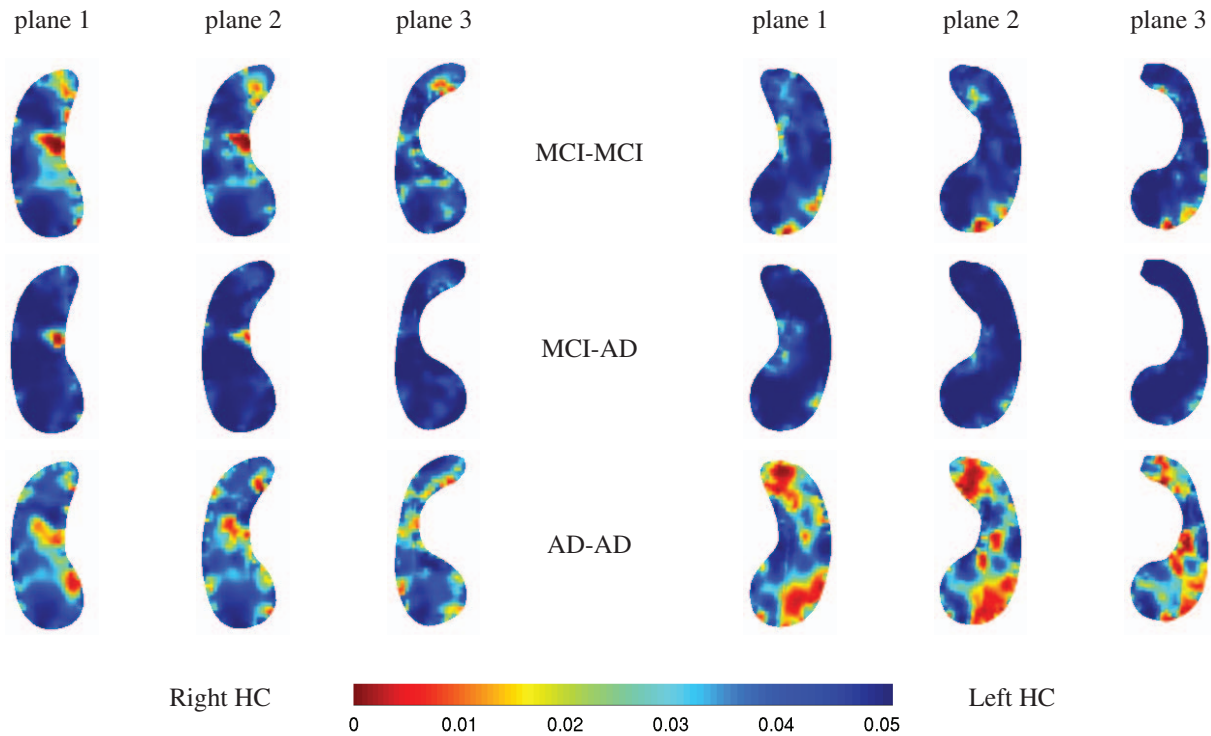


Fig. 1. Maps of p -values along 3 sections of the hippocampus.

5. SUMMARY AND DISCUSSION

We developed a Riemannian model of shape of solids in 3D space and applied it to the analysis of spatiotemporal evolution of hippocampal shape using longitudinal data comprising MR scans of the brain of 428 subjects collected by the ADNI at two points in time, one year apart. The analysis is based on geodesic interpolation of registered hippocampal volumes extracted from the baseline and follow-up scans of each subject. Analysis of regional morphological changes allowed us to identify specific regions of the hippocampus where shape changes due to neurodegeneration in conversion and progression of AD differs most significantly from normal aging over a 1-year period.

6. REFERENCES

- [1] J Barnes, JW Bartlett, LA van de Pol, CT Loy, RI Scahill, C Frost, PM Thompson, and NC Fox, "A meta-analysis of hippocampal atrophy rates in Alzheimer's disease," *Neurobiol Aging*, 2008.
- [2] J Morra, Z Tu, LG Apostolova, A Green, C Avedisian, S Madsen, N Parikshak, X Hua, A Toga, C Jack, N Schuff, MW Weiner, and PM Thompson, "Mapping hippocampal degeneration in 400 subjects with a novel automated segmentation approach," in *ISBI*, 2008.
- [3] J Morra, Z Tu, LG Apostolova, A Green, C Avedisian, S Madsen, N Parikshak, A Toga, C Jack, N Schuff, MW Weiner, PM Thompson, and the ADNI, "Automated mapping of hippocampal atrophy in 1-year repeat MRI data from 490 subjects with Alzheimer's disease, mild cognitive impairment, and elderly controls," *NeuroImage*, vol. 45, no. 1, pp. S3–S15, 2009.
- [4] SG Mueller, MW Weiner, LJ Thal, RC Petersen, C Jack, W Jagust, JQ Trojanowski, A Toga, and L Beckett, "The Alzheimer's disease neuroimaging initiative," *Clin. North Am.*, vol. 15, pp. 869–877 xi–xii, 2005.
- [5] X Liu, W Mio, Y Shi, and I Dinov, "Geodesic shape spaces of surfaces of genus zero," in *MICCAI*, 2008.
- [6] X Liu, Y Shi, J Morra, X Liu, PM Thompson, and W Mio, "Mapping hippocampal atrophy with a multi-scale model of shape," in *ISBI*, 2009.
- [7] Y Shi, PM Thompson, GI de Zubicaray, SE Rose, Z Tu, I Dinov, and AW Toga, "Direct mapping of hippocampal surfaces with intrinsic shape context," *NeuroImage*, vol. 37, no. 3, pp. 792–807, 2007.
- [8] G Wahba, *Spline Models for Observational Data*, SIAM, Philadelphia, PA, 1990.